Nanometer Scale Organization of Mixed Surfactin/Phosphatidylcholine Monolayers

Magali Deleu,* Michel Paquot,* Philippe Jacques,# Philippe Thonart,§ Yasmine Adriaensen,¶ and Yves F. Dufrêne¶

*Unité de Chimie Biologique Industrielle and #Unité de Bioindustrie, Faculté Universitaire des Sciences Agronomiques de Gembloux, Passage des Déportés, 2, B-5030 Gembloux; §Centre Wallon de Biologie Industrielle, Université de Liège, 4000 Liège; and ¶Unité de Chimie des Interfaces, Université catholique de Louvain, Place Croix du Sud 2/18, 1348 Louvain-la-Neuve, Belgium

ABSTRACT Mixed monolayers of the surface-active lipopeptide surfactin-C_{15} and of dipalmitoyl phosphatidylcholine (DPPC) were deposited on mica and their nanometer scale organization was investigated using atomic force microscopy (AFM) and x-ray photoelectron spectroscopy (XPS). AFM topographic images revealed phase separation for mixed monolayers prepared at 0.1, 0.25, and 0.5 surfactin molar ratios. This was in agreement with the monolayer properties at the air-water interface indicating a tendency of the two compounds to form bidimensional domains in the mixed systems. The step height measured between the surfactin and the DPPC domains was 1.2 ± 0.1 nm, pointing to a difference in molecular orientation: while DPPC had a vertical orientation, the large peptide ring of surfactin was lying on the mica surface. The N/C atom concentration ratios obtained by XPS for pure monolayers were compatible with two distinct geometric models: a random layer for surfactin and for DPPC, a layer of vertically-oriented molecules in which the polar headgroups are in contact with mica. XPS data for mixed systems were accounted for by a combination of the two pure monolayers, considering respective surface coverages that were in excellent agreement with those measured by AFM. These results illustrate the complementarity of AFM and XPS to directly probe the molecular organization of multicomponent monolayers.

INTRODUCTION

Surfactins are surface-active lipopeptides produced by *Bacillus subtilis* strains, which are cyclic heptapeptides containing a fatty acid chain (Kakinuma et al., 1969). They are attracting more and more attention in basic and applied research due to their high surface activity (Maget-Dana and Ptak, 1992a) and to their important biological properties, including antiviral, antibacterial, and hemolytic activities (Bernheimer and Avigad, 1970; Vollenbroich et al., 1997a,b). The biological activity of surfactin directly relies on its interactions with biomembranes; consequently, understanding the molecular interactions and mixing behavior of surfactin with phospholipids in thin films is of great importance. Interfacial properties measurements and molecular modeling approaches have provided valuable insight into the miscibility and molecular orientation of mixed surfactin/phospholipid monolayers; however, these methods do not provide direct information on the spatial organization of the monolayers.

Lipid monolayers prepared by the Langmuir-Blodgett (LB) technique are valuable models of biomembranes. In particular, transferring lipid films onto solid substrata offers the possibility to apply surface analysis techniques that cannot be used at the air/water interface or in solution. X-ray photoelectron spectroscopy (XPS) provides a direct chemical analysis of solid surfaces, with an analyzed depth of about 5 nm (Ratner and McElroy, 1986). Although XPS has been widely used to study the surface of materials, its application to probe the spatial organization of lipid LB monolayers has been limited (Solletti et al., 1996). During the last decade, atomic force microscopy (AFM) has emerged as a powerful tool for imaging the structure of supported lipid films (Egger et al., 1990; Weisenhorn et al., 1990; Zasadzinski et al., 1991; Hui et al., 1995; Mou et al., 1995; Solletti et al., 1996; Dufrêne et al., 1997). However, the use of AFM to study the organization of mixed surfactin/phospholipid monolayers has not yet been reported.

The aim of this paper is to gain insight into the spatial organization (miscibility, molecular orientation) of mixed surfactin/phosphatidylcholine monolayers. To this end, the morphology and chemical composition of the mixed monolayers transferred on mica are determined by AFM and XPS, respectively, and compared with the interfacial properties of the films at the air/water interface.

MATERIALS AND METHODS

Surfactin with a β-hydroxy fatty acid chain of 15 carbon atoms (molecular weight, 1036) was used in this study. It was produced and purified as described previously (Razafindralambo et al., 1998). Primary structure and purity of the surfactin-C_{15} (>95%) were ascertained by analytical RP-HPLC (Chromspher 5 μm C18 column, 1 × 25 cm, Chrompack, Middelburg, The Netherlands), amino acid analysis (Moore and Stein, 1951), and electrospray mass spectrometry (Finnigan MAT 900 ST) measurements.

LB monolayers were prepared at 20°C with an automated LB system (LFW2 3″5–Lauda, Königshofen, Germany). Surfactin and dipalmitoyl phosphatidylcholine (DPPC) purchased from Sigma Chemical Co. (St. Louis, MO) were dissolved at 1 mM in chloroform/methanol (2:1). Pure solutions and (0.1:0.9), (0.25:0.75), and (0.5:0.5) molar mixtures of surfactin and DPPC were spread on a milliQ water (Millipore Co., Milford, MA) subphase adjusted at pH 2.0 with HCl. After evaporation of the solvent, monolayers were compressed at a rate of 150 cm^2/min. They were

Received for publication 3 May 1999 and in final form 15 July 1999.

Address reprint requests to Yves Dufrêne, Tel.: 32-10-47-35-89; Fax: 32-10-47-20-05; E-mail: dufrene@cifa.ucl.ac.be.

0006-3495/99/10/2304/07 $2.00

deposited at a constant surface pressure of 20 mN/m, i.e., well below the collapse pressure, by raising vertically freshly cleaved mica through the air-water interface at a rate of 10 mm/min. The transfer ratios were all close to 1:1. For determining the compression isotherm curves, films were compressed at a rate of 61.8 cm^2/min. The difference between molecular areas of two independent sets of measurements was less than 2.5%.

AFM measurements were performed at room temperature (20°C) using a commercial optical lever microscope (Nanoscope III, Digital Instruments, Santa Barbara, CA). Contact mode topographic and friction images were recorded using oxide-sharpened microfabricated Si_3N_4 cantilevers (Park Scientific Instruments, Mountain View, CA) with typical radius of curvature of 20 nm and spring constants ranging from 0.01 N/m to 0.1 N/m. The imaging force was kept as low as possible (~1 nN) and the scan rate was 2 Hz.

XPS analyses were performed with an SSI X-Probe (SSX-100/206) photoelectron spectrometer from Fisons, interfaced with a Hewlett Packard 9000/310 computer allowing instrument control, data accumulation, and data treatment. The pressure during analysis was between 2.5×10^{-6} Pa and 2.5×10^{-7} Pa. The spectrometer used monochromatized Al K_α x-ray radiation (1486.6 eV). The irradiated zone was an elliptic spot, with a shorter axis of 1000 μm. The constant pass energy in the hemispherical analyzer was 150 eV or 50 eV. In these conditions, the resolution determined by the full width at half maximum of the $Au_{4f7/2}$ peak of a standard gold sample was about 1.5 and 1.0 eV, respectively. The flood gun energy was set to 8 eV and a nickel grid was placed 3 mm above the surface.

The following sequences of spectra were recorded: survey spectrum, C_{1s}, K_{2p}, O_{1s}, P_{2p}, Si_{2p}, Al_{2p}, N_{1s}, and finally C_{1s} again to check for the absence of sample degradation. Binding energies were determined by reference to the C_{1s} component due to carbon bound only to carbon and hydrogen, set at 284.8 eV. The background was subtracted linearly. Data treatment was performed with the ESCA 8.3 D software provided by the spectrometer manufacturer. Atom concentration ratios were calculated using the peak areas normalized on basis of acquisition parameters and of sensitivity factors proposed by the manufacturer (mean free path varying according to the 0.7th power of the photoelectron kinetic energy; Scofield cross-sections (Scofield, 1976); constant transmission function).

RESULTS

Fig. 1 shows the surface pressure-area (π-A) isotherms, at the air-water interface, of pure surfactin and DPPC monolayers, and of mixed surfactin/DPPC monolayers at 0.1, 0.25, and 0.5 surfactin molar ratios. At 20 mN/m, DPPC and surfactin occupy 46 and 142 $Å^2$/molecule, respectively. The mean area for mixed monolayers is always between those of pure monolayers.

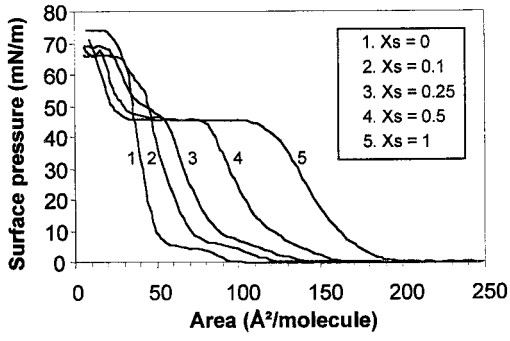

FIGURE 1 Surface pressure-area (π-A) isotherms, at the air-water interface, of pure surfactin and DPPC monolayers, and of mixed surfactin/DPPC monolayers at 0.1, 0.25, and 0.5 surfactin molar ratios recorded at 20°C with a water subphase at pH 2.0.

Fig. 2 shows AFM topographic and friction images of mixed surfactin/DPPC monolayers transferred on mica for 0.1, 0.25, and 0.5 surfactin molar ratios. All monolayers show phase separation, the shape and the size of the domains varying with the molar composition. For 0.1, 0.25 and 0.5 surfactin molar ratios, the area fraction covered by the lower (darker) domains in the topographic images is 26 ± 4%, 52 ± 6%, and 74 ± 3%, while the step height measured between the lower and higher domains is 1.2 ± 0.1 nm for the three molar ratios (mean values and standard deviations of height differences measured from cross-sections taken from three different images). The topographic and friction contrasts always show a negative correlation, higher friction being associated with the lower domains.

Fig. 3 presents the surface elemental composition determined by XPS for mixed surfactin/DPPC monolayers at 0.0, 0.1, 0.25, 0.5, and 1.0 surfactin molar ratios. Continuous changes of the surface composition occur with increasing surfactin molar ratios: the atom fractions of O_{1s}, N_{1s}, Si_{2p}, Al_{2p}, and K_{2p} increase concomitantly with a decrease in the C_{1s} and P_{2p} atom fractions. The concentrations of Si_{2p}, Al_{2p}, and K_{2p} are close to the 3:3:1 ratio expected for Muscovite mica.

Representative N_{1s} spectra for the pure and mixed monolayers, shown in Fig. 4, indicate that nitrogen is involved in different chemical functions depending on the surfactin molar ratio. For the pure surfactin monolayer, nitrogen appears at about 400 eV, which is attributable to unprotonated amine or amide functions (Gerin et al., 1995). In contrast, for the pure DPPC monolayer, nitrogen is observed at about 402 eV, which is typical of protonated amine (Gerin et al., 1995). The nitrogen peaks of mixed monolayers clearly show two components, attributed to unprotonated amine or amide functions (400 eV) and to protonated amine (402 eV), the contribution of the first component increasing with increasing surfactin molar ratios.

DISCUSSION

Interfacial properties at the air/water interface

The π-A isotherms of the pure surfactin and DPPC monolayers at the air-water interface (Fig. 1) are in agreement with those reported in previous studies (Marra, 1985; Maget-Dana and Ptak, 1992a,b). Their shape indicates that, at 20 mN/m, the DPPC monolayer is characterized by a two-dimensional solid-like organization, while surfactin has a two-dimensional liquid-like organization. The area of DPPC at 20 mN/m (46 $Å^2$) reflects a vertical, or slightly tilted, orientation of the lipid molecules (Marra and Israelachvili, 1985). In contrast, the large area of surfactin (142 $Å^2$) corresponds to an orientation in which the peptide ring is lying horizontally (Gallet et al., 1999). At higher surface pressure, the surfactin isotherm shows a horizontal plateau. Then, a sharp increase of surface pressure is observed at very low areas per molecule, corresponding to a condensed state in which the peptide cycles are probably

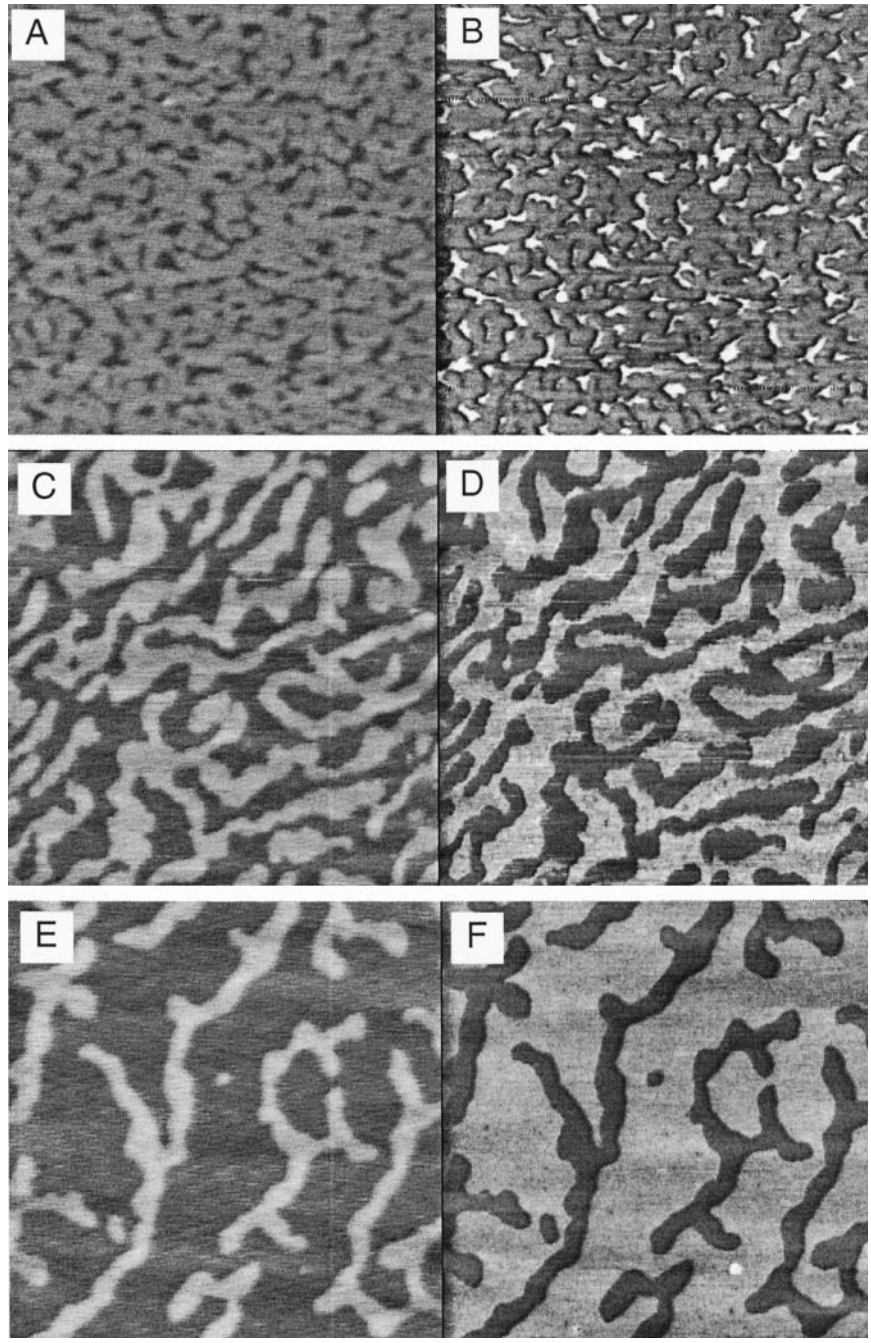

FIGURE 2 AFM topographic (*A, C, E*) and friction (*B, D, F*) images (2 × 2 μm) of mixed surfactin/DPPC monolayers at 0.1 (*A, B*), 0.25 (*C, D*), and 0.5 (*E, F*) surfactin molar ratios. The root-mean-square surface roughness of the two phases in the topographic images was ~0.1 nm (over 100 × 100 nm areas).

perpendicular to the interface (Maget-Dana and Ptak, 1992a).

To gain insight into the miscibility of surfactin and DPPC in mixed monolayers, the mean molecular area observed for the mixed films at 20 mN/m may be plotted against the molar fraction of surfactin (Gaines, 1966; Maget-Dana et al., 1989; Maget-Dana and Ptak, 1992b). The plot, presented in Fig. 5, shows small positive deviations from additivity for the mean molecular area, which suggests incomplete miscibility of the two compounds with the formation of bidimensional domains (Maget-Dana et al., 1989).

The interactions between surfactin and DPPC in mixed films may be further assessed by calculating the excess free energy of mixing ΔG_m^{ex} using the Goodrich relationship (Gaines, 1966; Maget-Dana and Ptak, 1995; Razafindralambo et al., 1997):

$$\Delta G_m^{ex} = \int_0^{\Pi} A_{12} d\Pi - x_1 \int_0^{\Pi} A_1 d\Pi - x_2 \int_0^{\Pi} A_2 d\Pi \qquad (1)$$

where A is the mean molecular area, x is the molar fraction, subscripts 1, 2, and 12 refer to pure compounds 1 and 2, and

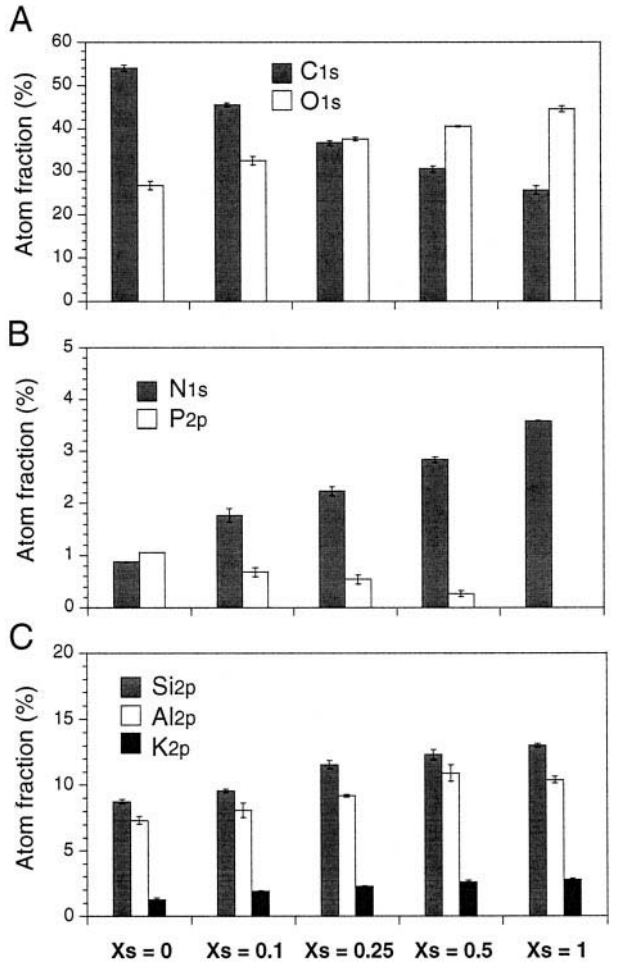

FIGURE 3 Surface chemical composition determined by XPS for pure surfactin and DPPC monolayers on mica and mixed surfactin/DPPC monolayers at 0.1, 0.25, and 0.5 surfactin molar ratios on mica. Atom fractions (%) of C_{1s} and O_{1s} (*A*), N_{1s} and P_{2p} (*B*), and Si_{2p}, Al_{2p}, and K_{2p} (*C*). *Bars*, difference between two independent sets of data.

to their mixtures, respectively. ΔG_m^{ex} values of 2.7, 3.1, and 3.4 are obtained for 0.1, 0.25, and 0.5 surfactin molar ratios, respectively. Thus, a positive excess of free energy of mixing is found for the three surfactin/DPPC monolayer systems, indicating that the interactions between lipopeptide and lipid molecules are weaker than the interactions between the pure compounds themselves. Accordingly, both the deviations from the additivity rule and the excess free energy of mixing suggest that surfactin and DPPC molecules have a tendency to form bidimensional domains in the mixed monolayers.

Surface morphology of mixed monolayers

AFM topographic images reveal phase separation for the three mixed surfactin/DPPC monolayers (Fig. 2). The area fraction occupied by the two domains may be compared with that expected for surfactin and DPPC in the mixed monolayer at the air-water interface (Fig. 1). Considering the surfactin molar ratio (X_s) and the areas occupied by the

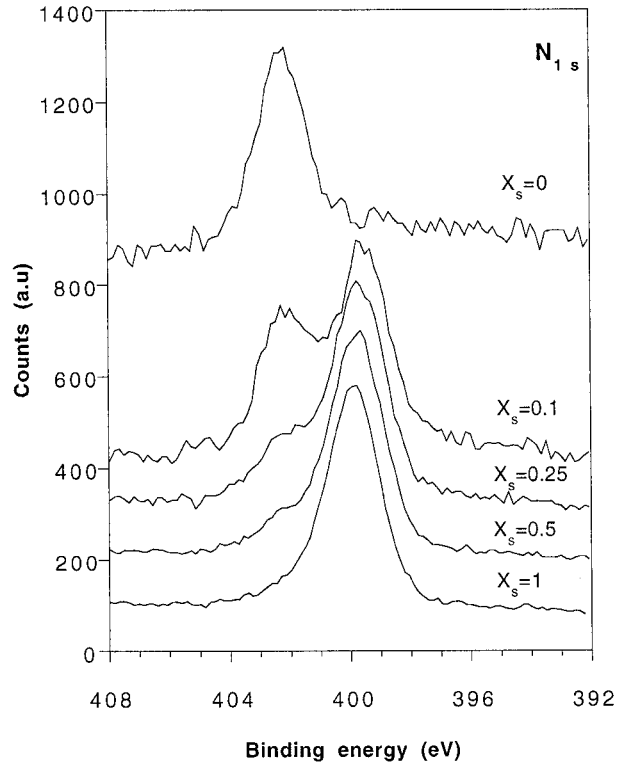

FIGURE 4 Representative N_{1s} spectra of mixed surfactin/DPPC monolayers on mica for surfactin molar ratios (*top* to *bottom*) of 0.0, 0.1, 0.25, 0.5, and 1.0.

surfactin and DPPC molecules in pure monolayers (A_s and A_d), the fraction of the surface occupied by surfactin in mixed monolayers at the air-water interface (γ) may be calculated as follows:

$$\gamma = \frac{X_s A_s}{(X_s A_s + (1 - X_s) A_d)} \quad (2)$$

At 20 mN/m, i.e., for $A_s = 142$ Å^2 and $A_d = 46$ Å^2, γ is found to be 0.26, 0.51, and 0.76, for $X_s = 0.1$, 0.25, and 0.5, respectively. The area fractions occupied by the lower domains in the AFM topographic images (26, 52, and 74, for

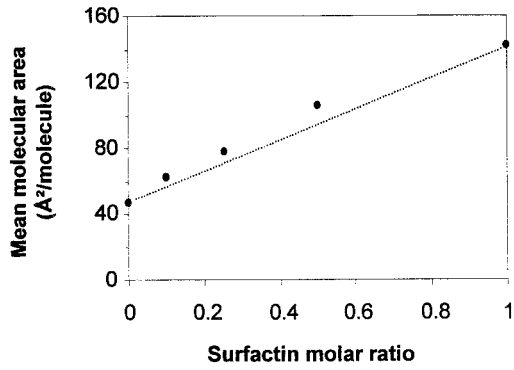

FIGURE 5 Mean molecular area of mixed surfactin/DPPC monolayers as a function of the surfactin molar ratio. The line represents the additivity rule values.

X_s = 0.1, 0.25, and 0.5, respectively) are in excellent agreement with the γ values calculated by Eq. 2. This indicates that: 1) the lower and higher levels in the AFM topographic images can be assigned to surfactin and DPPC, respectively; 2) surfactin and DPPC are completely immiscible in the conditions investigated here; 3) the molecular packing of the two compounds within the mixed monolayers is not significantly affected by transferring the films from the air/water interface onto mica.

The observation of phase separation for mixed surfactin/DPPC monolayers may be of biological importance. Previous studies have shown that the interactions of surfactin with biological membranes determine its antibacterial and antiviral action and involve insertion into the lipid bilayers, permeability changes probably resulting from ion channel formation, and membrane disruption at high surfactin concentrations (Sheppard et al., 1991; Thimon et al., 1993; Maget-Dana and Ptak, 1995; Vollenbroich et al., 1997a,b). The tendency of surfactin to self-associate and form bidimensional aggregates was proposed to be involved in channel formation. Hence, the small bidimensional domains of surfactin observed here at low concentration (X_s = 0.1) may play an important role in determining the surfactin biological activity.

The step height measured between the surfactin and DPPC domains in the topographic images may be related to the orientation assumed by the two compounds within the films. The thickness of the DPPC and surfactin monolayers (t) may be estimated from the molecular mass (M_w) and specific mass (d) of the compounds, the Avogadro constant (N_{av}) and the area at the air-water interface at the deposition pressure of 20 mN/m (A):

$$t = M_w/d \times A \times N_{av} \quad (3)$$

Considering d = 1 g/cm^3 gives a monolayer thickness of 2.6 nm and 1.2 nm for DPPC and surfactin, respectively. The thickness deduced for DPPC is in good agreement with that reported from refractive index measurements (Marra and Israelachvili, 1985). The step height measured by AFM, 1.2 $\pm$ 0.1 nm, is close to the difference between the computed thicknesses, 1.4 nm. Since the two compounds have fairly similar molecular lengths, the large difference in film thicknesses observed by AFM provides direct evidence for a difference in molecular configuration; while DPPC assumes a vertical (or slightly tilted) orientation (Marra and Israelachvili, 1985), the large peptide ring of surfactin is lying on the mica surface. This is consistent with a recent molecular modeling study which showed that the more stable structure for surfactin at a hydrophobic/hydrophilic interface corresponds to the peptide ring positioned in the plane of the interface with the fatty acid chain folded to interact with the aminoacids (Gallet et al., 1999).

A significant contrast in friction is observed (Fig. 2), despite the presence of alkyl chain ends for both compounds. The friction contrast may originate from a difference in molecular packing within the films: compared to the closely packed DPPC alkyl chains, the molecular disorder of the surfactin alkyl chains may give rise to higher friction. On the other hand, the higher friction on the surfactin domains may also reflect higher surface energy, compared to DPPC, due to the exposure of polar amino acids at the surface.

Spatial organization of pure and mixed monolayers

XPS brings further information on the spatial organization of the monolayers. Since both nitrogen and carbon are characteristic of the biological overlayers, but not of mica, N/C ratios determined by XPS for pure monolayers, (N/C)xps, may be compared with N/C ratios deduced from the stoichiometric composition, (N/C)sto, of surfactin ($C_{53}O_{13}N_7H_{93}$) and DPPC ($C_{40}O_6N_1P_1H_{80}$). For the pure surfactin monolayer, a good agreement is found between the two ratios: (N/C)xps = 0.14 and (N/C)sto = 0.13. Hence, the XPS data fit with a random overlayer model, i.e., a model in which surfactin is not vertically oriented (Fig. 6 *A*). This model is consistent with the molecular configuration deduced from the AFM images. The agreement between the experimental and stoichiometric N/C ratios also indicates that the concentration of carbon originating from organic contamination is negligible.

In contrast, for the pure DPPC monolayer, the (N/C)xps ratio (0.016) is significantly lower than the (N/C)sto ratio (0.025) suggesting that the contribution of nitrogen is attenuated due to the presence of an overlayer. To gain further insight into the spatial organization of the film, the XPS data

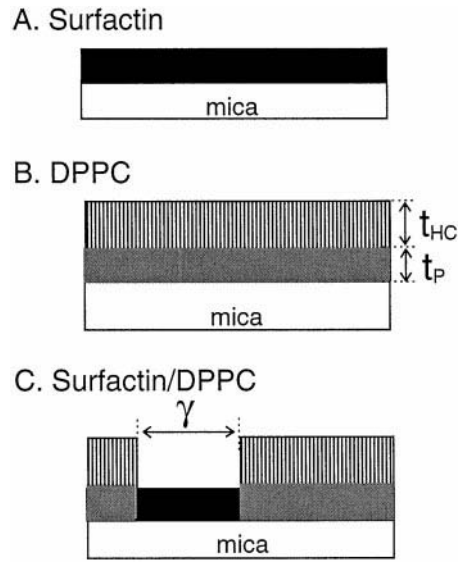

FIGURE 6 Geometric models considered for interpreting XPS data. (*A*) surfactin monolayer; (*B*) DPPC monolayer; (*C*) mixed surfactin/DPPC monolayer. The surfactin monolayer is modeled as a homogeneous layer. The DPPC monolayer is modeled as an inner polar layer of thickness t_P and an outer hydrocarbon layer of thickness t_{HC}. Mixed monolayers are modeled as combinations of the two above models; the fraction of the surface occupied by surfactin is γ.

may be interpreted considering that the pure DPPC monolayer consists of a double layer, i.e., an inner polar layer of thickness t_P and an outer hydrocarbon layer of thickness t_{HC} (Fig. 6 *B*). The apparent N/C ratio expected from XPS is given by:

$$\frac{N}{C} = \frac{i_C}{i_N}\frac{\sigma_N}{\sigma_C}\left(\frac{\lambda_N^P C_N^P[1 - \exp(-t_P/\lambda_N^P \cos\theta)]\exp(-t_{HC}/\lambda_N^{HC}\cos\theta)}{\lambda_C^{HC}C_C^{HC}[1 - \exp(-t_{HC}/\lambda_C^{HC}\cos\theta)] + \lambda_C^P C_C^P[1 - \exp(-t_P/\lambda_C^P \cos\theta)]\exp(-t_{HC}/\lambda_C^{HC}\cos\theta)}\right) \quad (4)$$

where i_C (1.00) and i_N (1.68) are the sensitivity factors for carbon and nitrogen, respectively; σ_C (1.0) and σ_N (1.8) are the Scofield cross-sections (Scofield, 1976); λ represents the inelastic electron mean free path in the polar layer (λ_N^P = 3.2 nm and λ_C^P = 3.5 nm; Andrade, 1985) or in the hydrocarbon layer (λ_N^{HC} = 3.6 nm and λ_C^{HC} = 3.9 nm; Andrade, 1985); C_N^P and C_C^{HC} are the concentrations of nitrogen and carbon in the polar (C_N^P = 3.2 mmol cm^{-3}) and hydrocarbon (C_C^{HC} = 76.8 mmol cm^{-3}) layers; θ is the take-off angle measured between the normal to the sample surface and the direction of photoelectron collection, i.e., 55°.

Fig. 7 shows the variation of the apparent N/C ratio calculated from Eq. 4 as a function of the polar (t_p) and hydrocarbon (t_{HC}) layer thicknesses. The experimental N/C ratio of 0.016 is compatible with different pairs of (t_P, t_{HC}) values. Considering a t_P value of 0.7 nm, estimated from the volume occupied by the DPPC head group, i.e., 0.324 nm^3 (Marra and Israelachvili, 1985), and the area occupied at the air-water interface, gives a best value for t_{HC} of about 1.5 nm and thus a total thickness of 2.2 nm, which is in satisfactory agreement with the expected DPPC film thickness. This observation supports the validity of the double layer model for the DPPC film, i.e., a model of vertically oriented molecules in which the polar headgroups are in contact with mica (Fig. 6 *B*). It also points to the fact that the level of carbonaceous contamination at the surface is low. Note that a variation of 25% on t_{HC} or t_P values would cause a variation of about 25% on the apparent N/C ratio (Fig. 7), indicating that the sensitivity of the results to the data precision is appreciable.

Mixed monolayers may be modeled as a combination of the two pure monolayers (Fig. 6 *C*), the apparent N/C ratio being computed as follows:

$$\frac{N}{C} = \frac{\gamma N_{surfactin} + (1 - \gamma)N_{dppc}}{\gamma C_{surfactin} + (1 - \gamma)C_{dppc}} \quad (5)$$

where γ is the fraction of the surface occupied by surfactin; $N_{surfactin}$, N_{dppc}, $C_{surfactin}$, and C_{dppc} represent the apparent nitrogen and carbon atom fractions determined by XPS on pure surfactin and pure DPPC monolayers. Fig. 8 shows the apparent N/C ratios, computed from Eq. 5, as a function of γ. As can be seen, experimental values of N/C and γ determined by XPS and AFM for surfactin molar ratios of 0.1, 0.25, and 0.5 fit well with the above combined model. Hence, the XPS data for the mixed systems are accounted for by a combination of the two pure monolayers, considering respective surface coverages that are in excellent agreement with those measured by AFM. In this work, LB monolayers were prepared at a low surface pressure (20 mN/m), which corresponds to surfactin peptide rings lying horizontally. In further studies, it could be interesting to focus on the spatial organization of mixed monolayers

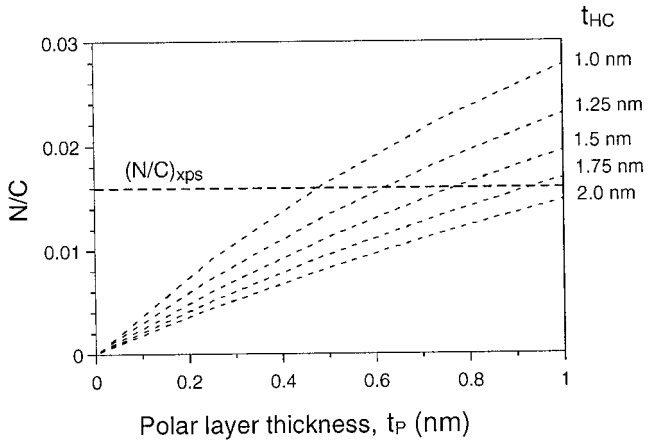

FIGURE 7 Variation of the apparent N/C ratios computed for the pure DPPC monolayer (Eq. 4) as a function of t_P for t_{HC} of 1.0, 1.25, 1.5, 1.75, and 2.0 nm. The horizontal line shows the N/C ratio determined by XPS.

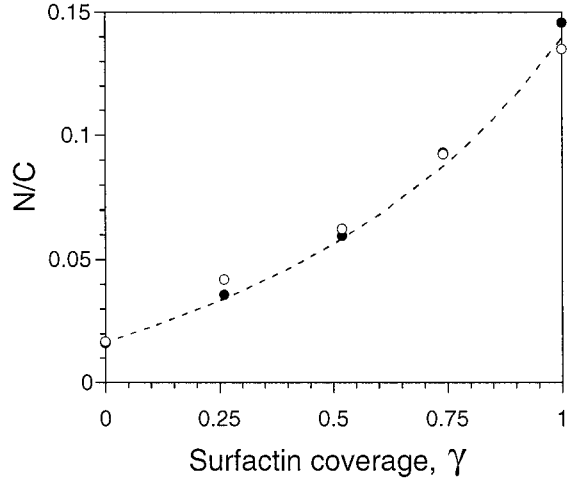

FIGURE 8 Variation of N/C ratio as a function of the surfactin surface coverage (γ) for the mixed monolayers. *Open* and *closed circles* are two independent sets of experimental data. The line shows the apparent N/C ratios computed from Eq. 5.

transferred at higher surface pressures (e.g., 50 mN/m), in relation with cell and liposome membrane properties.

CONCLUSION

Although the miscibility and the interactions of biologically active lipopeptides with lipids have been studied for many years, direct information at high spatial resolution was not available. In this study, phase separation is directly visualized by AFM for mixed surfactin/DPPC monolayers on mica at 0.1, 0.25, and 0.5 surfactin molar ratios. The observation of bidimensional domains is consistent with the monolayer properties at the air-water interface. The fraction of the surface occupied by the two domains indicate complete immiscibility of the two compounds. AFM height measurements and modeling of the XPS data provide direct and independent pieces of evidence for the molecular orientation of the two compounds within the monolayers; while DPPC assumes a vertical orientation with the polar head groups in contact with mica, the large peptide ring of surfactin is lying on the mica surface. This work has promising applications in biophysics for the direct characterization of the spatial organization (domain formation, molecular orientation) of multicomponent monolayers and adsorbed phases.

M. D. thanks the FNRS for her position as Research Assistant. The authors thank Prof. P. Grange for the use of the atomic force microscope and P. G. Rouxhet, M. Rosch, and C. Robert for valuable discussions.

The support of the National Foundation for Scientific Research (FNRS), of the Federal Office for Scientific, Technical and Cultural Affairs (Interuniversity Poles of Attraction Programme), and of the European Union (BIO4-CT950176) is gratefully acknowledged.

REFERENCES

Andrade, J. D. 1985. X-ray photoelectron spectroscopy (XPS). *In* Surface and Interfacial Aspects of Biomedical Polymers, Vol. 1, Surface Chemistry and Physics. J. D. Andrade, editor. Plenum Press, New York. 105–195.

Bernheimer, A. W., and L. S. Avigad. 1970. Nature and properties of a cytolytic agent produced by *Bacillus subtilis*. *J. Gen. Microbiol.* 61: 361–369.

Dufrêne, Y. F., W. R. Barger, J.-B. D. Green, and G. U Lee. 1997. Nanometer-scale surface properties of mixed phospholipid monolayers and bilayers. *Langmuir*. 13:4779–4784.

Egger, M., F. Ohnesorge, A. L. Weisenhorn, S. P. Heyn, B. Drake, C. B. Prater, S. A. C. Gould, P. K. Hansma, H. E. Gaub. 1990. Wet lipid-protein membranes imaged at submolecular resolution by atomic force microscopy. *J. Struct. Biol.* 103:89–94.

Gaines, G. L. 1966. Mixed monolayers. *In* Insoluble Monolayers at Liquid-Gas Interfaces. I. Prigogine, editor. Intersciences Publishers/New York, London, Sydney. 281–300.

Gallet, X., M. Deleu, H. Razafindralambo, P. Jacques, P. Thonart, M. Paquot, and R. Brasseur. 1999. Computer simulation of surfactin conformation at a hydrophobic/hydrophilic interface. *Langmuir*. 15: 2409–2413.

Gerin, P. A., P. B. Dengis, and P. G. Rouxhet. 1995. Performance of XPS analysis of model biochemical compounds. *J. Chim. Phys.* 92: 1043–1065.

Hui, S. W., R. Viswanathan, J. A. Zasadzinski, and J. N. Israelachvili. 1995. The structure and stability of phospholipid bilayers by atomic force microscopy. *Biophys. J.* 68:171–178.

Kakinuma, A., A. Ouchida, T. Shima, H. Sugino, H. Isono, G. Tamura, and K. Arima. 1969. Confirmation of the structure of surfactin by mass spectrometry. *Agric. Biol. Chem.* 33:1669–1671.

Maget-Dana, R., and M. Ptak. 1992a. Interfacial properties of surfactin. *J. Colloid Interface Sci.* 153:285–291.

Maget-Dana, R., and M. Ptak. 1992b. Surfactin: interfacial properties and interactions with membrane lipids in mixed monolayers. *Thin Solid Films.* 210/211:730–732.

Maget-Dana, R., and M. Ptak. 1995. Interactions of surfactin with membrane models. *Biophys. J.* 68:1937–1943.

Maget-Dana, R., I. Harnois, and M. Ptak. 1989. Interactions of the lipopeptide antifungal iturin A with lipids in mixed monolayers. *Biochim. Biophys. Acta*. 981:309–314.

Marra, J. 1985. Controlled deposition of lipid monolayers and bilayers onto mica and direct force measurements between galactolipid bilayers in aqueous solutions. *J. Colloid Interface Sci.* 107:446–458.

Marra, J., and J. Israelachvili. 1985. Direct measurements of forces between phosphatidylcholine and phosphatidylethanolamine bilayers in aqueous electrolyte solutions. *Biochemistry*. 24:4608–4618.

Moore, S., and W. Stein. 1951. Aminoacid determination, methods and techniques. *J. Biol. Chem.* 192:663–670.

Mou, J., J. Yang, and Z. Shao. 1995. Atomic force microscopy of cholera toxin B-oligomers bound to bilayers of biologically relevant lipids. *J. Mol. Biol.* 248:507–512.

Ratner, B. D., and B. J. McElroy. 1986. Electron spectroscopy for chemical analysis: applications in the biomedical sciences. *In* Spectroscopy in the Biomedical Sciences. R. M. Gendreau, editor. CRC Press, Boca Raton, FL. 107–140.

Razafindralambo, H., Y. Popineau, M. Deleu, C. Hbid, P. Jacques, P. Thonart, and M. Paquot. 1997. Surface-active properties of surfactin/iturin A mixtures produced by *Bacillus subtilis*. *Langmuir*. 13: 6026–6031.

Razafindralambo, H., Y. Popineau, M. Deleu, C. Hbid, P. Jacques, P. Thonart, and M. Paquot. 1998. Foaming properties of lipopeptides produced by *Bacillus subtilis*: effect of lipid and peptide structural attributes. *J. Agric. Food Chem.* 46:911–916.

Scofield, J. H. 1976. Hartree-Slater subshell photoionization cross-sections at 1254 and 1487 eV. *J. Electron Spectrosc. Relat. Phenom.* 8:129–137.

Sheppard, J. D., C. Jumarie, D. G. Cooper, and R. Laprade. 1991. Ionic channels induced by surfactin in planar lipid bilayer membranes. *Biochim. Biophys. Acta.* 1064:13–23.

Solletti, J. M., M. Botreau, F. Sommer, W. L. Brunat, S. Kasas, T. Minh Duc, and M. R. Celio. 1996. Elaboration and characterization of phospholipid Langmuir-Blodgett films. *Langmuir*. 12:5379–5386.

Thimon, L., F. Peypoux, J. Wallach, and G. Michel. 1993. Ionophorous and sequestering properties of surfactin, a biosurfactant from *Bacillus subtilis*. *Colloids Surfaces B: Biointerfaces.* 1:57–62.

Vollenbroich, D., M. Özel, J. Vater, R. M. Kamp, and G. Pauli. 1997a. Mechanism of inactivation of enveloped viruses by the biosurfactant surfactin from *Bacillus subtilis*. *Biologicals.* 25:289–297.

Vollenbroich, D., G. Pauli, M. Özel, and J. Vater. 1997b. Antimycoplasma properties and application in cell culture of surfactin, a lipopeptide antibiotic from *Bacillus subtilis*. *Appl. Env. Microbiol.* 63:44–49.

Weisenhorn, A. L., B. Drake, C. B. Prater, S. A. C. Gould, P. K. Hansma, F. Ohnesorge, M. Egger, S.-P. Heyn, and H. E. Gaub. 1990. Immobilized proteins in buffer imaged at molecular resolution by atomic force microscopy. *Biophys. J.* 58:1251–1258.

Zasadzinski, J. A. N., C. A. Helm, M. L. Longo, A. L. Weisenhorn, S. A. C. Gould, and P. K. Hansma. 1991. Atomic force microscopy of hydrated phosphatidylethanolamine bilayers. *Biophys. J.* 59:755–760.